

**Final Report:** Measuring the degree of connectivity between remnant staghorn patches at risk of anthropogenic impacts

**Grant number:** NOAA Coral Reef Conservation Grant NA12NOS4820071

**Program Officer:** Liz Fairey ,[301.427.8632](tel:301.427.8632), [liz.fairey@noaa.gov](mailto:liz.fairey@noaa.gov)

**Program Office:** NOS Office of Ocean and Coastal Resource Management (OCRM)

**Amount of grant:** \$74,680

**PI's:** Jennifer McIlwain and Laurie Raymundo, The University of Guam, UoG Marine Lab, Mangilao, GU 96923

**Award Period:** 08/01/2012 - 02/28/2015 (Extension granted)

## EXECUTIVE SUMMARY

Utilising a suite of techniques which combined population genetics with bio-physical and larval dispersal modelling we test the relative influence of connectivity in remote island populations of a Staghorn coral, *Acropora pulchra*. This species is confined to the shallow lagoons around the reef flats of Guam and adjacent islands in the southern end of the Mariana Archipelago. Total population size of this species has been reduced over the past decade through a combination of bleaching events and pollution, and its long term future in the archipelago remains unclear. Mapping of staghorn corals on Guam revealed a total area of 33 ha across 14 reef-flat and lagoon locations. *Acropora pulchra* was the dominant species making up 90% of the total area. More than 50% of all Guam's staghorn corals were found in Tumon Bay, followed by West Agana (19.3%) and Agat (14.7%). The analysis of 8 microsatellite loci from 430 staghorn colonies collected across multiple sites within Guam and Saipan, revealed high levels of asexual fragmentation at distances >30m ; one of the widest spreads among other coral species similarly analyzed. Bayesian clustering analysis and migration modeling uncovered a putative dispersal barrier between staghorn corals in Cocos Lagoon at the southern tip of Guam and staghorn patches along Guam's entire West coast. The most parsimonious migration model indicated that the Cocos Lagoon population does not contribute enough migrants per generation to the remainder of Guam to maintain genetic homogeneity. A secondary barrier was also evident between Guam and Saipan to the north, albeit not at the same level as the Cocos Lagoon. Fish species assemblages inside and outside of *Acropora* thickets were similar across the three locations with the greatest coral cover; Tumon, East Agana and Agat. Our bio-physical modelling showed larvae spawned at the two locations with greatest *A.pulchra* cover (Tumon Bay and Agana Bay) were most likely to settle long the northwest coast with no chance of settlement south of Orote Point. Similarly those spawned at Agat were retained along the southwest coast or advected westwards. For the Cocos Lagoon population the dispersal modelling supports that of the genetics results whereby larvae spawned from Cocos do not settle elsewhere on Guam. The small *A.pulchra* population on the east coast at Togcha make no contribution to larval settlement on the west coast with most larvae advected to the south of the island. A recent bleaching event during the summer months of 2014, at the latter stages of the project, gave us the opportunity to run our anticipated modelling scenario's as "real" events. We found that when adult mortality was reduced by up to 70%, larval settlement was heavily impacted and proportional to the loss of adults. To determine whether marine preserves act to "reseed" adjacent non-protected areas we found only one Marine Preserve on Guam, Tumon Bay acts as a net exporter of *Acropora* staghorn larvae. We argue that while asexual propagation (the dominant mode of reproduction for *A.pulchra* on Guam) is a successful strategy for responding to storm disturbances, a lack of external larval supply leaves local populations prone to extinction, especially under a regime of increasing SST's

and greater frequency of bleaching. Such restricted gene flow within an island only 35 miles long and 5 miles wide was surprising but is consistent with the apparent lack of resilience being displayed by extant staghorn populations.

## **INTRODUCTION**

As a result of human population increases along coastal margins, coral communities worldwide have undergone major deleterious changes for many decades. While significant gains have recently been made in conserving and more effectively managing areas of coral reef the world has effectively lost 19 % of the original area of coral reefs, with another 15% seriously threatened within the next 10-20 years and a further 20% under threat of loss in the next 20-40 years (Wilkinson 2008). Global warming is now compounding the situation through increased coral bleaching and outbreaks of coral disease, along with increased cyclonic activity and acidification of our oceans (Hoegh-Guldberg et al. 2007). While local to regional-scale management cannot directly ameliorate the global-scale effects of climate change they can still ensure their existing reef populations are as healthy and resilient as possible as we move into an uncertain climate future.

However, the effective management of coral reef resources at local to regional scales requires detailed knowledge of the population dynamics of those organisms at risk. One such group are the staghorn corals (genus *Acropora*) of Guam. These species commonly form thickets or patches and are confined to the inner reef-flat-zone moats and lagoons where water is retained at low tide (Randall 1973, Randall et al. 1975). This dependence on a narrow habitat type exposes these corals to an array of disturbances, including bleaching, coral diseases, sedimentation and other land-based sources of pollution; and physical damage from cyclonic waves and trampling (Burdick et al. 2008). Historical information on staghorn corals around Guam is limited, with total population size for this group unclear. Although, recent surveys of several sites along Guam's northwest coast show acroporids (*Acropora muricata* and *Acropora azurea*) comprise 5-35% of reef flat coral communities (Raymundo et al. 2011). Additionally, coral reef monitoring efforts by this same research group has found some staghorn coral patches recovered from bleaching while others have suffered significant and irreversible mortality (Ypao Beach, Tumon Bay; L. Raymundo unpub. data). Detailed information on the extent and life-history of local staghorn populations is therefore urgently needed; not only for ecological but also economic reasons. A recent assessment of the total economic value of Guam's coral reefs puts a dollar value of more than \$120 million per year (van Beukering et al. 2007). The aesthetic appeal of Guam's coral reefs attracts more than one million tourists annually, contributing 20% of island GDP and creating many thousands of jobs (Burdick et al. 2008).

The ongoing health of Guam's staghorn corals is also imperative for those organisms that rely on corals for food and shelter. While it's well known that staghorn *Acropora* corals are a primary food source and habitat for many reef fish, the impact from the loss of these corals can cause cascading effects throughout an entire reef fish community. Following a catastrophic loss of branching corals in Kimbe Bay, PNG it was found that the actual decline in abundance and diversity of coral reef fish was significantly greater than expected, based

on the total number of fish species that had an obligate association with coral. For example, while only 11% of the more than 500 fish species surveyed were coral specialists, nearly 75% of all fish species suffered a concomitant decline with branching coral over a seven year period (Jones et al. 2004). Species which depended on branching corals as recruitment sites had the greatest loss and several coral-specialists went locally extinct (Jones et al. 2004). Reef flats in general and more specifically reef flat areas with coral cover are primary recruitment zones and nursery areas for reef fish (Green 1994) and hence their integrity must be maintained. The proposed project will expand our knowledge of the life-history and population dynamics of staghorn corals around Guam. This is being achieved through the updating of existing baseline information (contained in the Guam Habitat Atlas) and the input of this data to a recently developed bio-physical model.

### **ACROPORA DISTRIBUTION**

Remote sensing techniques used to develop the distribution maps have been described elsewhere (Burdick 2005). Ground validation surveys were used to supplement the satellite imagery and performed by towing an observer behind a boat who subsequently mapped *Acropora* thickets using a hand-held GPS receiver.

**Table 1:** Total area of *Acropora* spp and *Acropora pulchra* mapped across 14 locations on Guam. For *A. pulchra* percentage of total area is given in brackets.

Location	Total <i>Acropora</i> m <sup>2</sup>	<i>A. pulchra</i> m <sup>2</sup> (%)	Other dominant spp
Tumon	151423	150056 (99.1)	
Tanguisson	6523	6482 (99.3)	
Double Reef	234	0 (0)	<i>A. acuminata</i>
Togcha	5035	5035 (100)	
Cocos Sth	21338	1 (<0.1)	<i>A. aspera</i> , <i>A. acuminata</i>
Cocos Nth	853	506 (59)	<i>A. muricata</i>
Agat	49140	43309 (88)	<i>A. muricata</i>
Gabgab	391	0 (0)	<i>A. austera</i> , <i>A. vaughni</i>
Apra Shoals	1257	0 (0)	<i>A. austera</i> , <i>A. muricata</i> , <i>A. virgata</i>
Luminao	890	0 (0)	<i>A. virgata</i>
Piti	485	33 (7)	<i>A. acuminata</i> , <i>A. muricata</i> <i>A. virgata</i> ,
Asan-Adelup	3221	3221 (100)	
West Agana	64372	64372(100)	
East Agana	27952	27952 (100)	
<b>TOTAL</b>	<b>333114</b>	<b>300967 (90)</b>	

Using a combination of remote sensing and field-based validation, 333 114 m<sup>2</sup> or 33.3 ha of *Acropora* thickets were mapped and quantified across 14 locations on Guam (Table 1). Of this total area *A.pulchra* was the dominate species comprising 90% or covering 300 967 m<sup>2</sup> or 30.97 ha. Tumon had approximately 50% of Guam's *Acropora* thickets, where more than 99% comprised of *A.pulchra* (Figure 1). West Agana and Agat had the next highest proportion of *Acropora*, with 64 372 and 43 309 m<sup>2</sup> respectively, again dominated by the one species *A.pulchra* (Figure 2,3). Like West Agana, East Agana had 100% coverage of its significant 27 952 m<sup>2</sup> of staghorn comprised of *A.pulchra* (Figure 4). Only Sth Cocos Lagoon had significant non-*A.pulchra* thickets where 21 338 m<sup>2</sup> of mostly *A.aspera* and *A.acuminata* occurred (Figure 5).

Staghorn patches in Piti, Luminao, Apra and Double Reef were insignificant and made up of small, remant thickets of other non-*A.pulchra* species including *A. acuminata*, *A.austera*, *A.vaughni* and *A.virgata* (Figure 6-14).

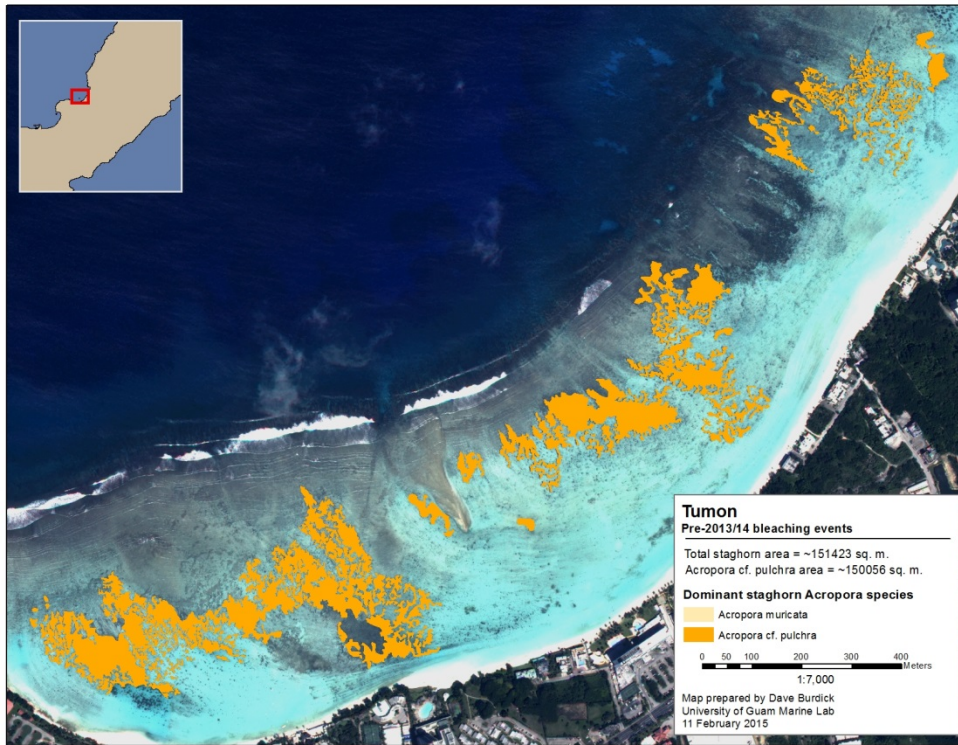


**Figure 1:** Satellite image showing total staghorn area that was mapped using remote sensing and field-based surveys for Tumon Bay, Guam.

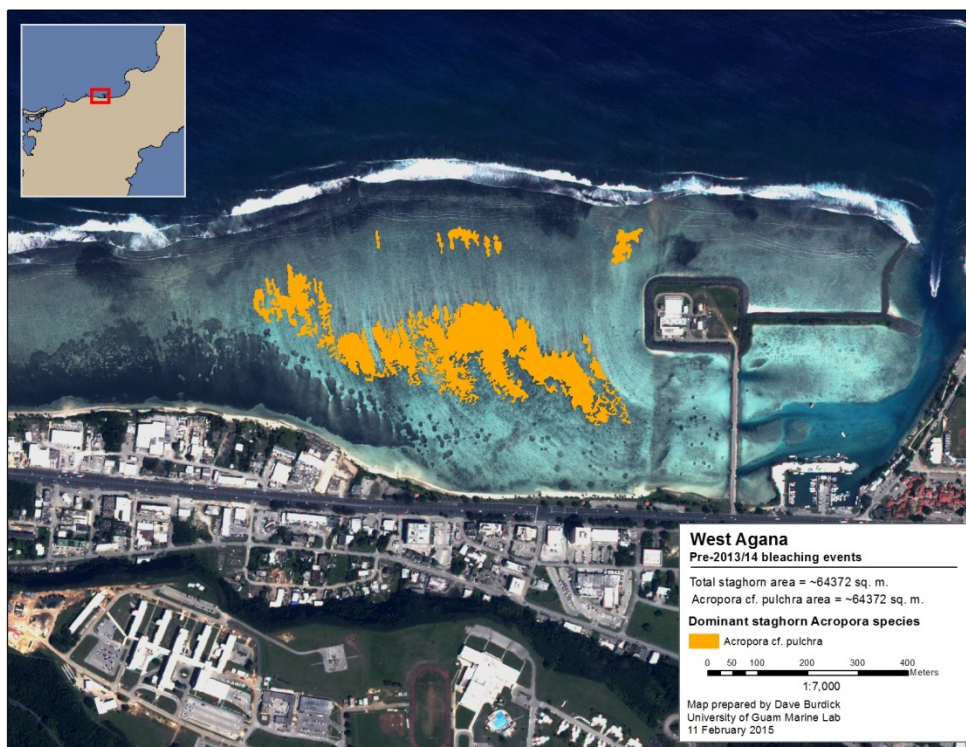


**Figure 2:** Satellite image showing total staghorn area that was mapped using remote sensing and field-based surveys for West Agana Bay, Guam.



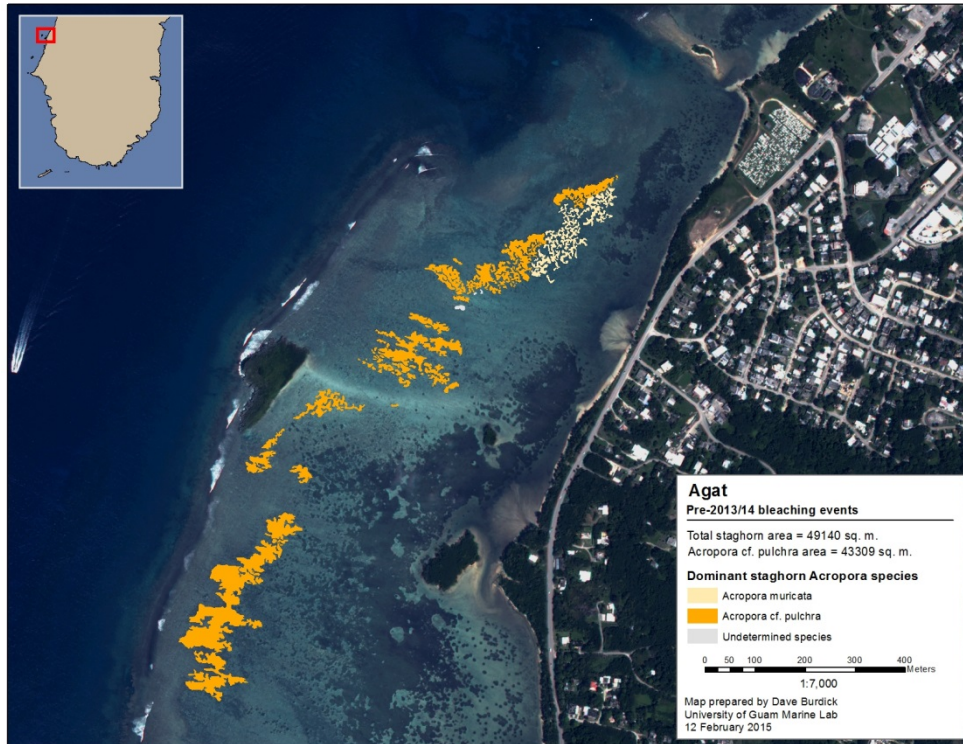


**Figure 3:** Satellite image showing total staghorn area that was mapped using remote sensing and field-based surveys for Agat, Guam.

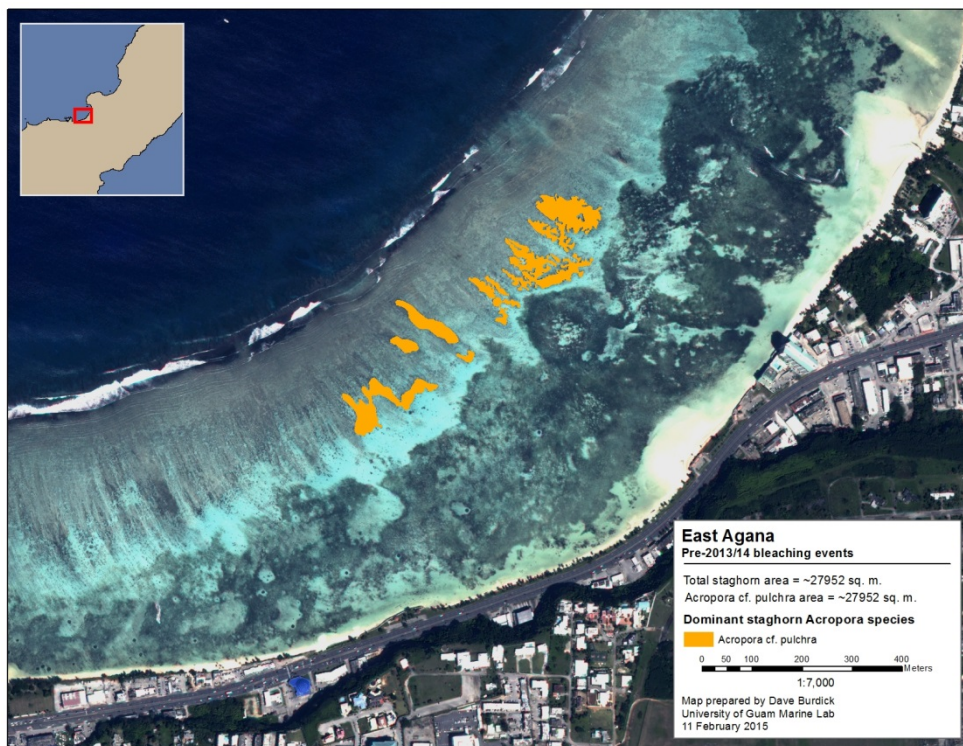


**Figure 4:** Satellite image showing total staghorn area that was mapped using remote sensing and field-based surveys for East Agana, Guam.



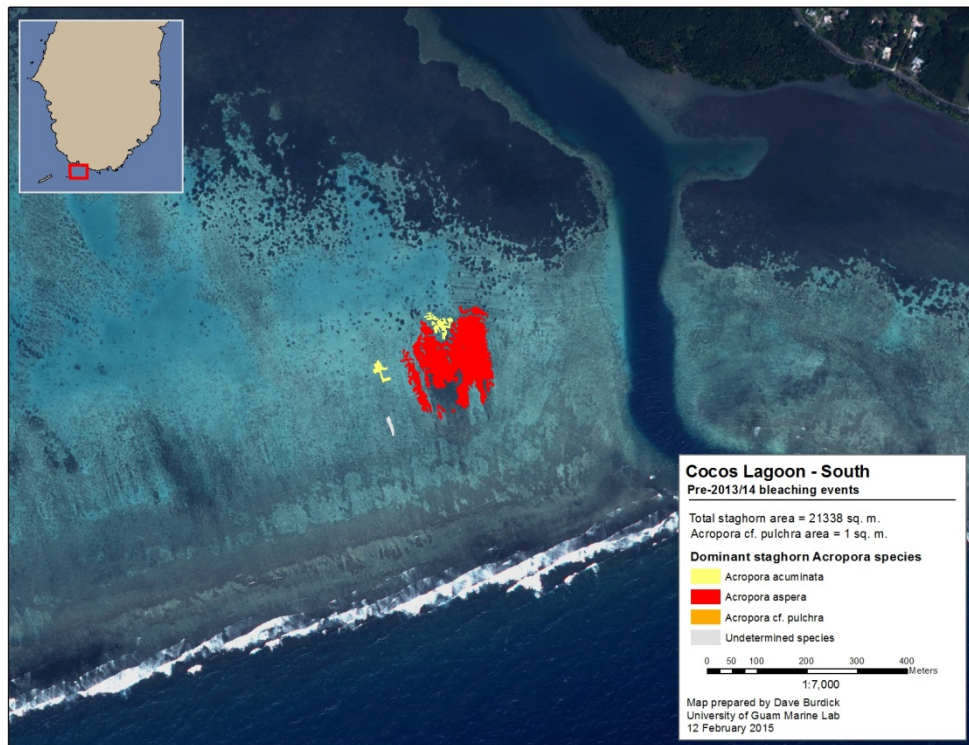


**Figure 5:** Satellite image showing total staghorn area that was mapped using remote sensing and field-based surveys for South Cocos Lagoon, Guam.

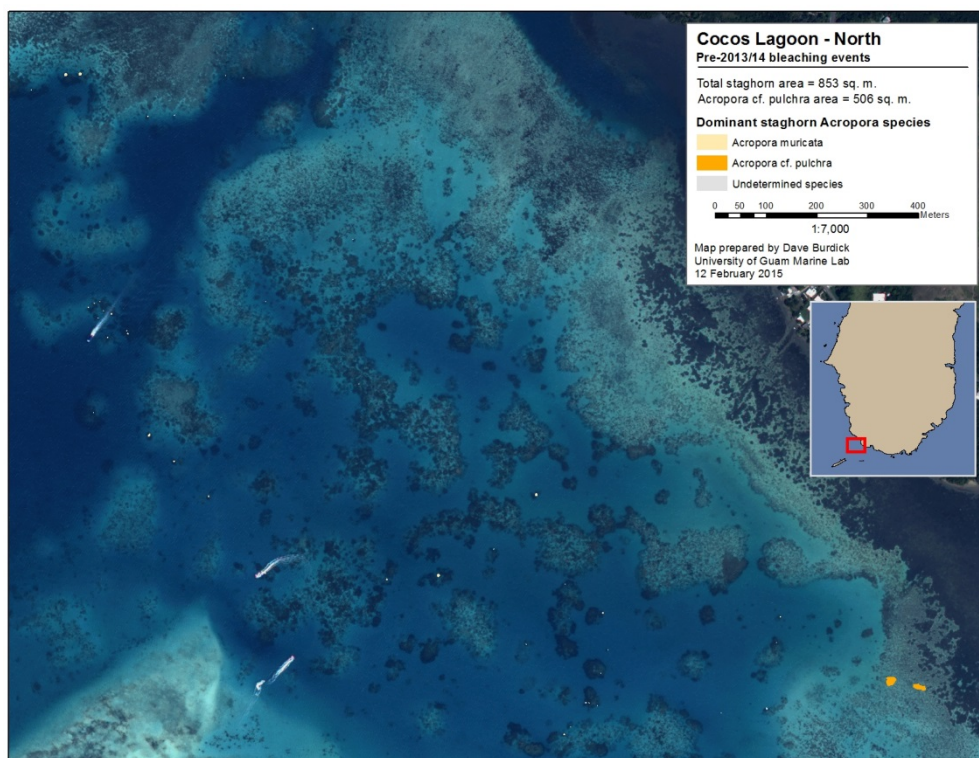


**Figure 6:** Satellite image showing total staghorn area that was mapped using remote sensing and field-based surveys for North Cocos Lagoon, Guam.

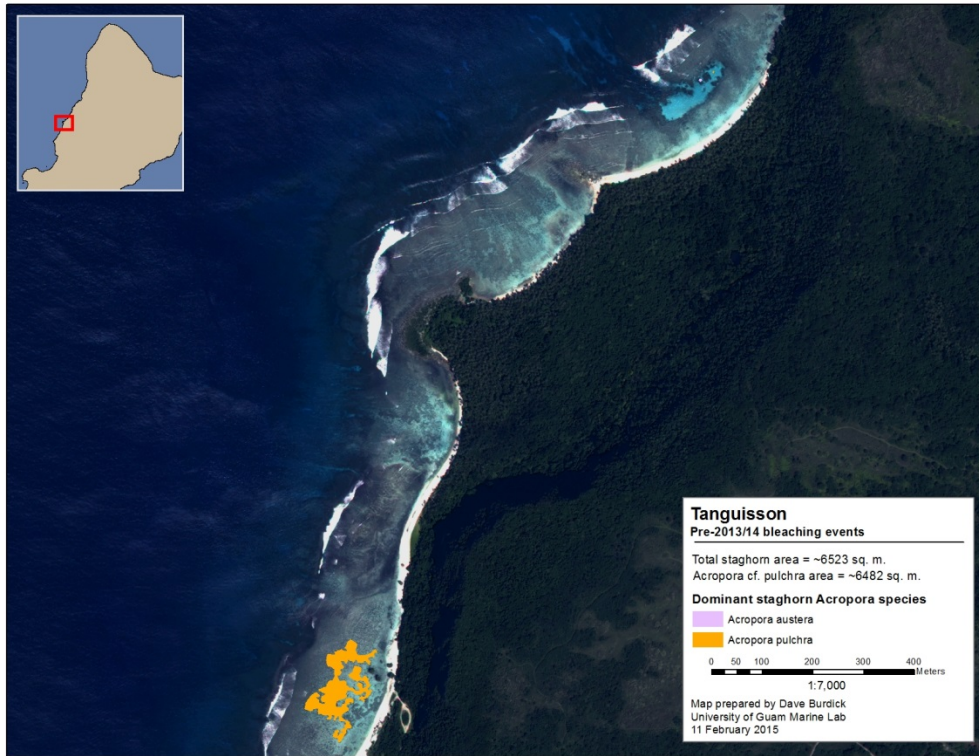


**Figure 7:** Satellite image showing total staghorn area that was mapped using remote sensing and field-based surveys for Tanguisson, Guam.

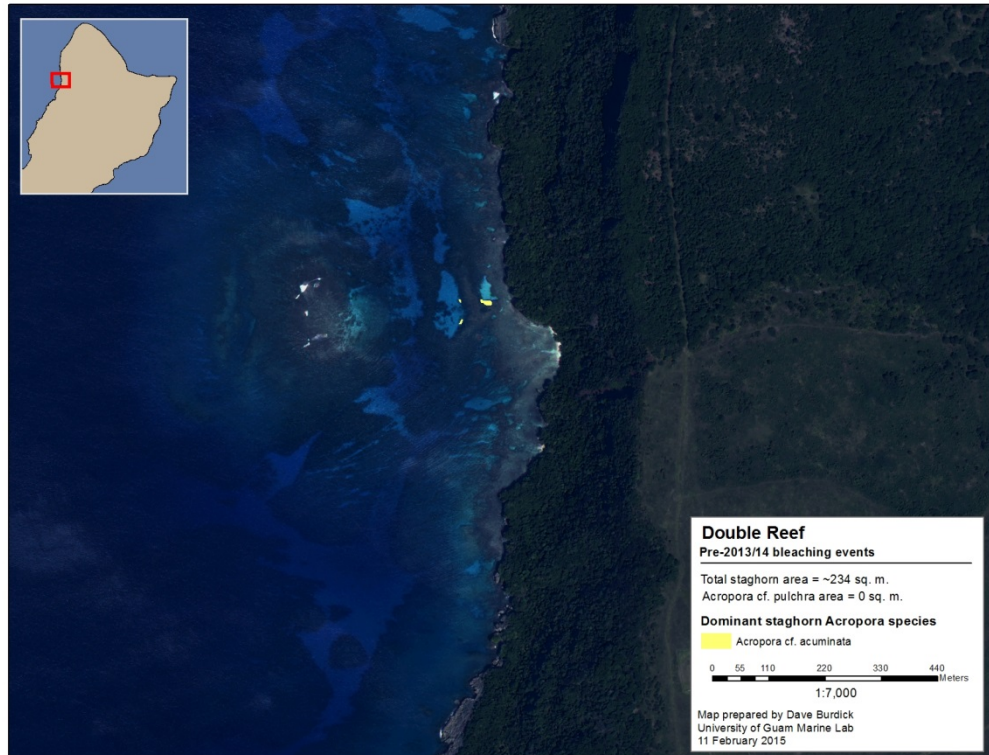


**Figure 8:** Satellite image showing total staghorn area that was mapped using remote sensing and field-based surveys for Double Reef, Guam.



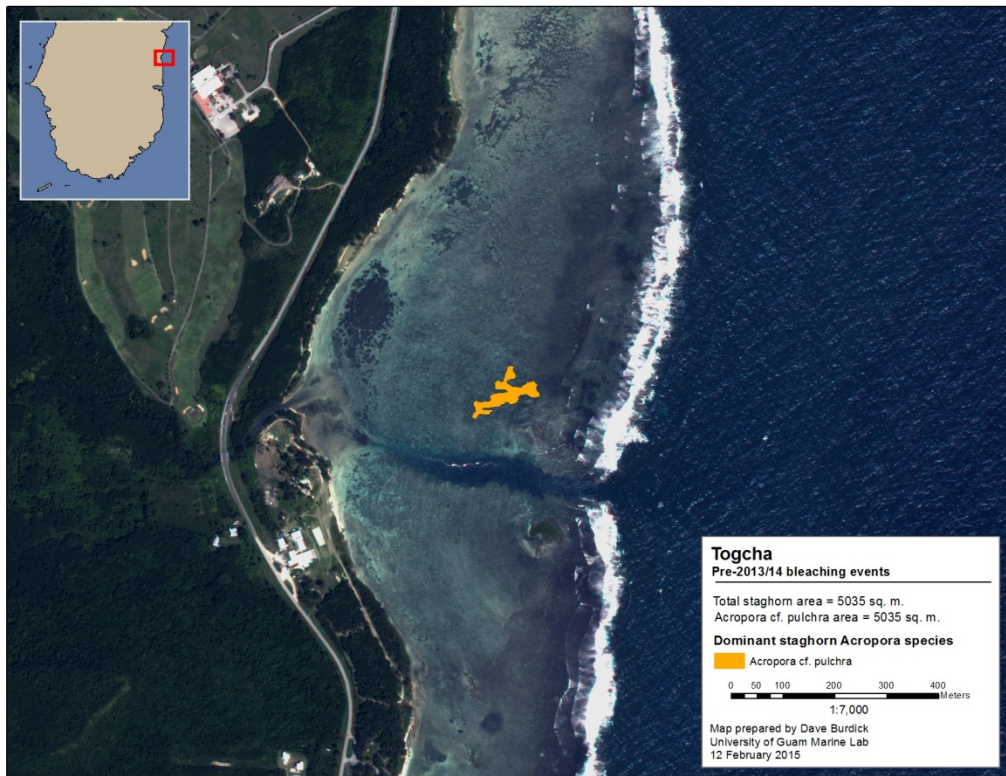


**Figure 9:** Satellite image showing total staghorn area that was mapped using remote sensing and field-based surveys for Togcha, Guam.



**Figure 10:** Satellite image showing total staghorn area that was mapped using remote sensing and field-based surveys for Gabgab, Guam.

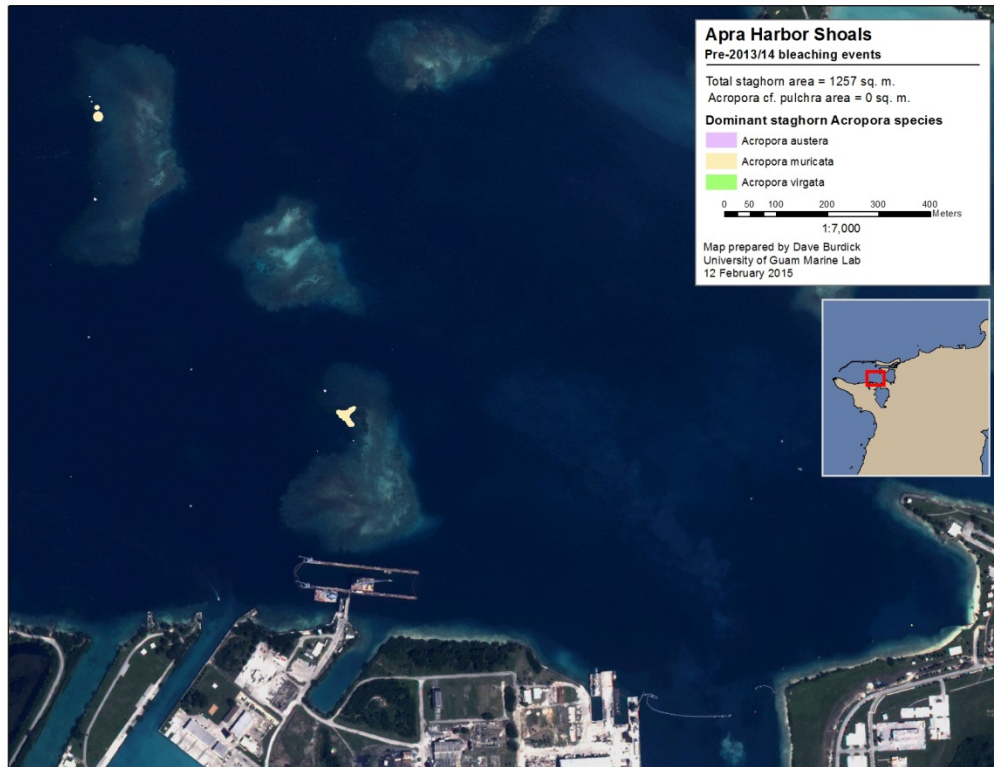


**Figure 11:** Satellite image showing total staghorn area that was mapped using remote sensing and field-based surveys for Apra Harbor, Guam.

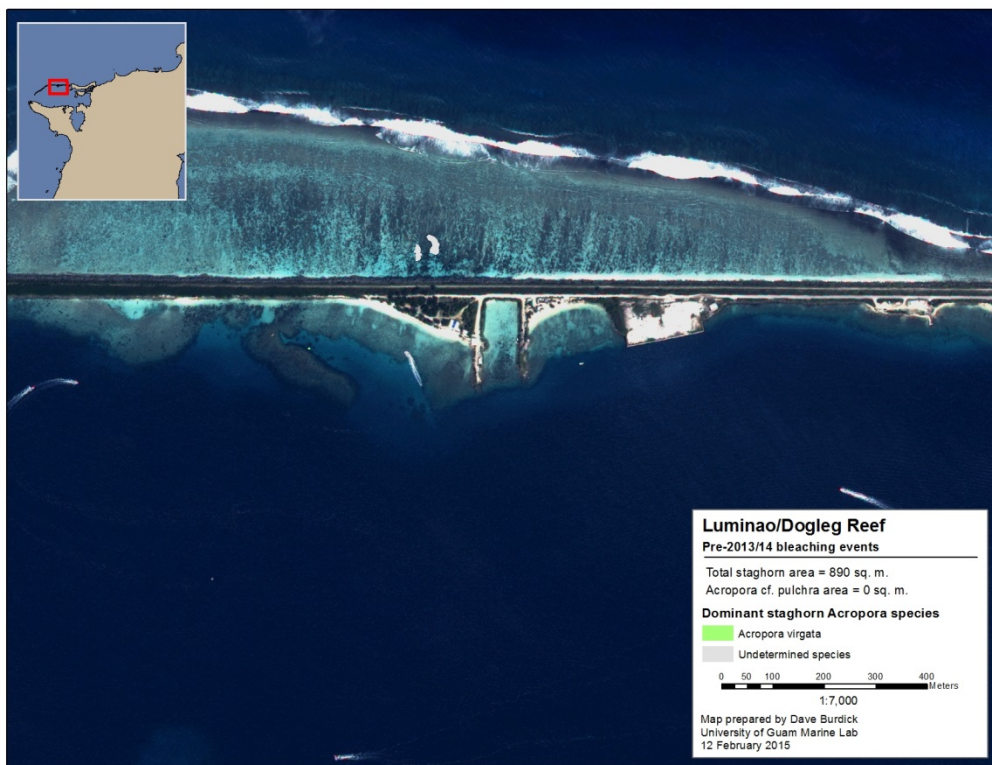


**Figure 12:** Satellite image showing total staghorn area that was mapped using remote sensing and field-based surveys for Luminao, Guam.



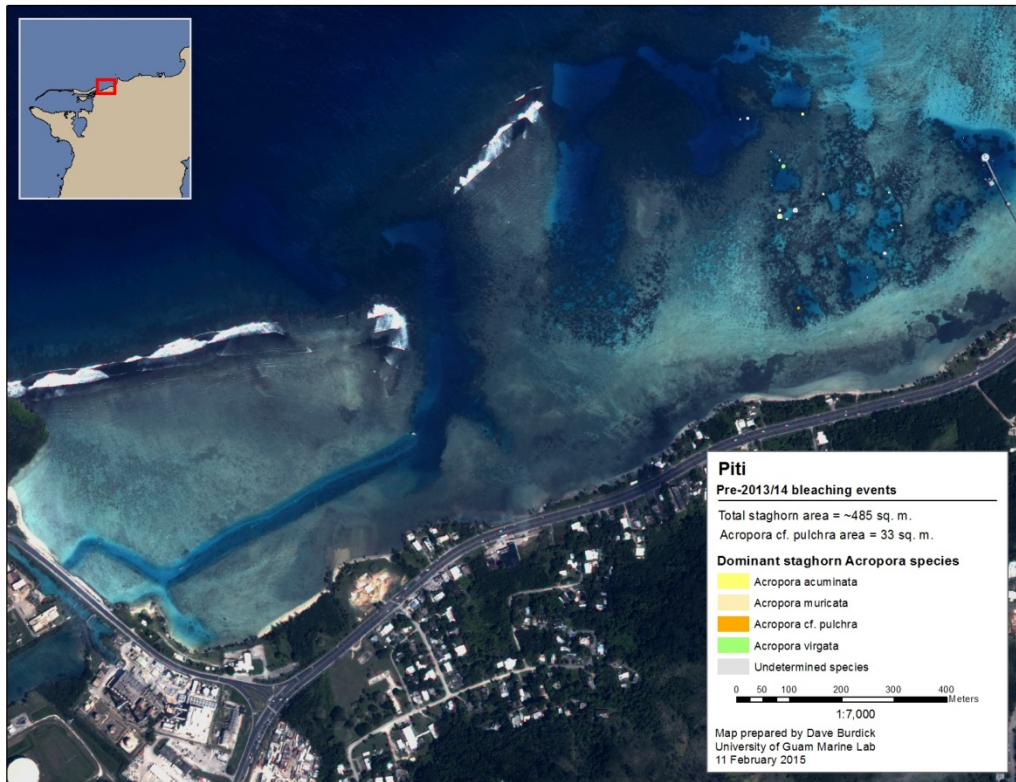


**Figure 13:** Satellite image showing total staghorn area that was mapped using remote sensing and field-based surveys for Piti, Guam.

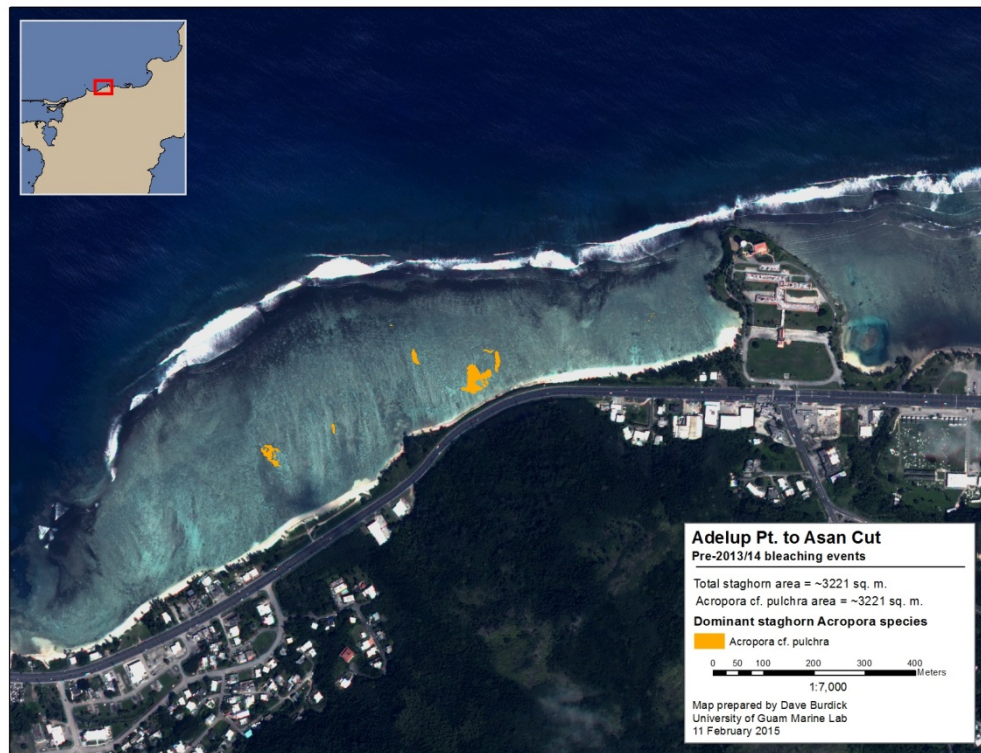


**Figure 14:** Satellite image showing total staghorn area that was mapped using remote sensing and field-based surveys for Adelup Point to Asan Cut, Guam.



## GENETIC DIVERSITY

### Genotyping

Methods for the genotyping, clonal structure, population structure and migration modelling can be found in the most recent progress report submitted on December 30, 2014.

A total of 399 *A. cf. pulchra* adults were sampled from 12 sites around Guam and 30 individuals were sampled from Saipan (Table 2). Failures in amplification resulted in the removal of 12 samples from the analysis and reduced the sample size to n=387. The average number of alleles (A) ranged from  $4.1 \pm 0.6$  to  $5.6 \pm 0.7$  at all sites except Cocos Lagoon where allelic diversity was lower ( $A=2.4 \pm 0.3$ ; Diversity Index=  $0.68 \pm 0.12$ ; Table 2). Although tests of HWE revealed that 4 of 8 loci were in HWE for all sites, significant deviations from HWE were evident in 10 out of the 54 tests (after correction for multiple testing) mainly at locus 166 and locus 180 (heterozygote excess).

**Table 2:** GPS coordinates, sampling method and number of *Acropora cf. pulchra* sampled and genotyped at each sampling site. After genotyping individuals missing data at >3 loci were removed ( $N_M$ ). The number of unique genotypes ( $N_G$ ) by sampling location is also given. GPS locations in decimal degrees.

Site	GPS	Sampling Method	N	$N_M$	$N_G$
<b>Agat</b>					
	N 13.38328, E 144.65231	Random	30		7
		Haphazard	9	1	4
	N 13.37637, E 144.64642	Random	30		9
<b>*Asan</b>					
	N 13.47692, E 144.72046	Random	30		4
	N 13.47953, E 144.72806	Haphazard	30		9
<b>Cocos Lagoon</b>					
	N 13.25112, E 144.67667	Random	30		7
<b>*E. Hagatna</b>					
	N 13.48538, E 144.76701	Random	30		8
<b>*W. Hagatna</b>					
	N 13.47948, E 144.74541	Random	30		7
<b>Tanguisson</b>					
	N 13.54803, E 144.81023	Random	30		7
<b>Luminao</b>					

	N 13.46463, E 144.64723	Haphazard	30		15
<b>Tumon</b>					
	N 13.50605, E 144.78826	Random	30	2	9
	N 13.51274, E 144.79962	Random	30	4	11
	N 13.50943, E 144.79683	Random	30	3	11
<b>Saipan</b>	N 15.17779, E 145.75097 approximate	Haphazard	30	2	19
<b>total: 9 sites</b>		10 random plots	399	12	127

\*grouped together for population genetic analyses

Null allele testing in MICROCHECKER suggested that locus 166 and 181 contained null alleles for all sites. However, the program INEST, which accounts for inbreeding and genotyping errors when estimating null alleles, found significant null alleles at locus 166 in 5 of the 7 sites, at locus 181 only at Saipan, and locus 1\_4 in Tumon. At locus 166, the additional 2 sites exhibited non-significant but high null allele frequencies (>0.1). Similarly, null allele frequencies were evident at some sites at locus 181, locus 53, and locus 1\_4 (Table 2).

Estimated inbreeding levels were low ( $\text{Avg}(F_i) < 0.035$  for all sites) and all 95% confidence intervals (CI) included 0 when using the full model in INEST (nfb; including null alleles (n), inbreeding (f), and genotyping errors(b)). At all sites, the model assuming null alleles and genotyping errors outperformed the full model including inbreeding (DIC values  $\text{nb} < \text{nfb}$ ) but the model assuming only inbreeding and genotyping errors performed worse than the full model (DIC values  $\text{fb} > \text{nfb}$ ). At Cocos both the “nb” and the “fb” model outperformed the “nfb” model but no deviations from HWE were observed. Under a maximum likelihood model in RMES, no site showed evidence for a significantly non-zero selfing rate based on both the 95% CI and hypothesis testing comparing the likelihood (lnl) value of the estimated selfing rate under an unconstrained model to the lnl under a constrained selfing rate =0 (chi-square,  $\text{df}=1, p > 0.2$  at sites).

### ***Clonal structure***

High levels of fragmentation were observed within our spatially explicit random sample collection (mean  $N_G/N = 0.28 \pm 0.1$  SD). Fragmentation rates varied from 0.13 to 0.46 among sites. The three plots sampled within Tumon Bay had the highest clonal richness (mean  $N_G/N = 0.4 \pm 0.07$  SD). The lone plot at Asan Bay had the lowest. On average, each genet comprised 4 ramets  $\pm 1.5$  SD within plots and therefore markedly reduced our sample size for further analysis (overall  $N=387$ ;  $N_G=127$ ). Even where sampling was conducted

haphazardly and intentionally biased against clones, repeated sampling of genotypes was common (i.e. Luminao  $N_G/N = 15/30$ ; see discussion of spatial extent of clonality). Between plots within the same site only one colony (Tumon N) shared a MLG ( $P_{sex}$  p-value < 0.001) with colonies from a separate plot (Tumon S). In this case, ramets were separated by a mean distance of  $1.44 \pm 0.005$  km. No other MLGs were shared between plots within or between sites. Excluding the previous case, maximum clonal extent ranged from 4.3 to 26.4 m with a global average of  $16.3 \pm 6.3$  m.

The spatial structure within a given plot was not significantly autocorrelated except at Agat S, where the distribution of clones exhibited high spatial aggregation (Table 3.  $A_c = 0.5$ ; Figure 15B), and W. Hagatna, where the majority of sampling occurred within 6 m from the center point (Figure 15D). Pairwise heterogeneity tests (Table 5-5) thus indicated that the spatial structure of genetic distance at Agat S was significantly different from the other 9 plots but no other significant differences were found between plots. The lack of spatial autocorrelation within plots was likely due to the random distributions of ramets (i.e. Asan and Tumon S) or a prevalent clone with a large spatial extent (i.e. E. Hagatna, Cocos; see Fig. 5-2).

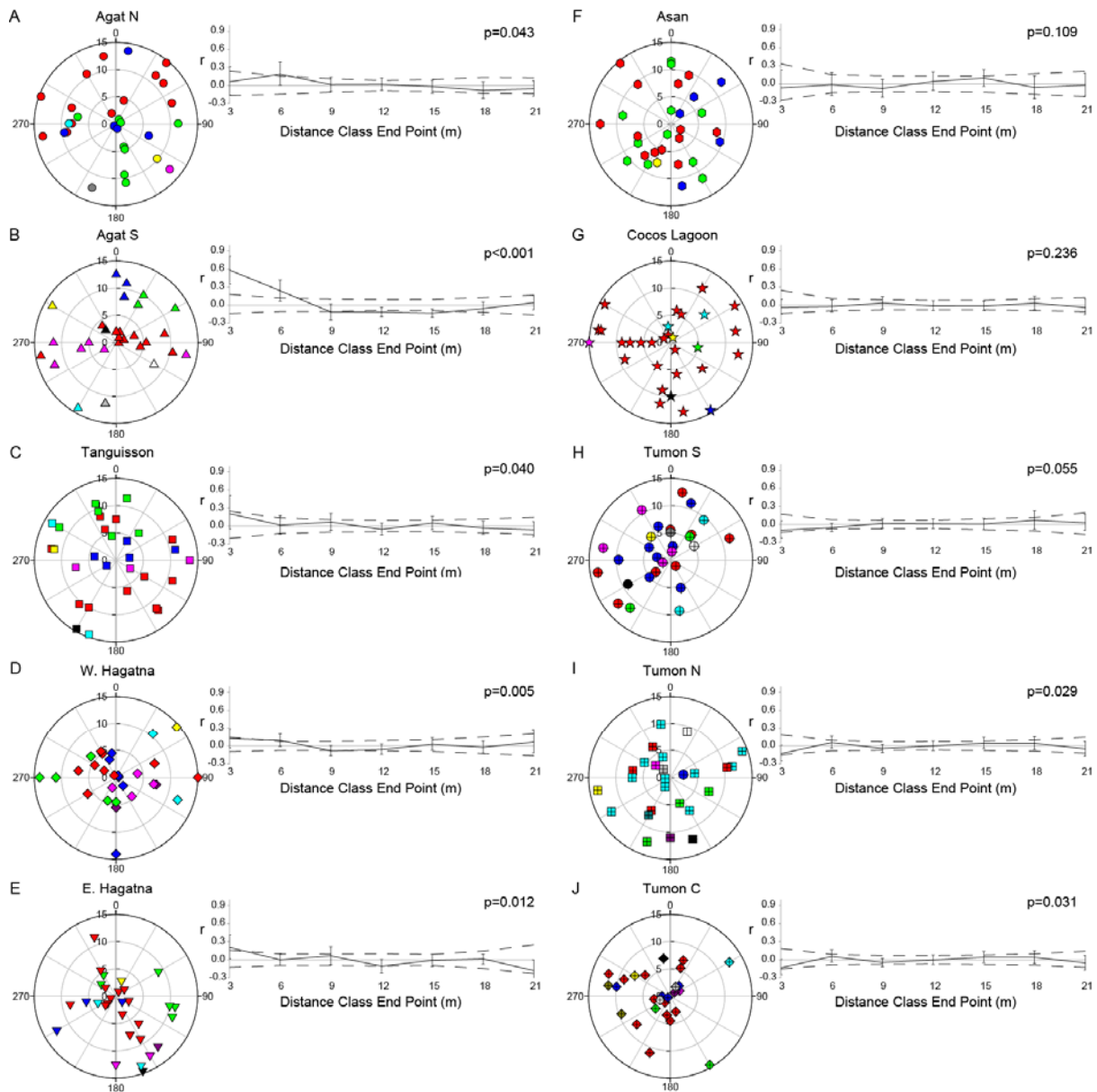


**Figure 15:** Left: 15m radius circular plots mapping the location and genotype of each *Acropora cf. pulchra* colony randomly sampled in the plot. Symbol and color combinations indicate individual genotypes. One genotype was repeated between plots (indicated by red arrows). Right: Correlograms, resulting from a spatial autocorrelation analysis within plots, which depict the correlation coefficient ( $r$ ) plotted against geographic distance with 7 distance classes of 3m (solid line). Dashed lines represent 95% confidence intervals about the null hypothesis of no spatial genetic structure (i.e. genotypes are distributed randomly across geographic space). Correlograms are considered to be significant at  $p < 0.01$  following (Banks & Peakall 2012).

**Table 3.** Indices of clonal structure as calculated for each polar plot. Sample size (N), the number of unique MLGs ( $N_G$ ), clonal richness ( $N_G/N$ ), genotypic diversity ( $G_O/G_E$ ), genotypic evenness ( $G_O/N_G$ ), the average number of ramets (R) per genet (G) is given as well as the average distance between clonemates (Genet Spread), the average maximum linear extent of each genet (Clonal Extent)

meters, the average clonal identity for all pairwise comparisons ( $P_{sg}$ ), the average clonal identity of nearest neighbor ( $P_{sp}$ ), the aggregation coefficient ( $A_c$ ), and the reef status. SD = standard deviation.

Site	N	N <sub>G</sub>	N <sub>G</sub> /N	G <sub>O</sub> /G <sub>E</sub>	G <sub>O</sub> / N <sub>G</sub>	R/G	Genet Spread (SD)	Clonal Extent (SD)	P <sub>sg</sub> <sup>1</sup>	P <sub>sp</sub> <sup>1</sup>	A <sub>c</sub> <sup>1</sup>	Reef Status <sup>2</sup>
Agat												
Agat N	30	7	0.23	0.11	0.49	4.29	11.39(5.99)	21.25(4.37)	0.73	0.50	0.32	fair
Agat S	30	9	0.30	0.15	0.49	3.33	7.42(5.98)	12.97(10.36)	0.79	0.40	0.50	fair
Tanguisson	30	7	0.23	0.14	0.58	4.29	11.53(5.6)	18.94(3.92)	0.78	0.70	0.10	good
*Hagatna												
W Hagatna	30	7	0.23	0.17	0.71	4.29	7.75(5.56)	14.02(5.56)	0.83	0.57	0.32	varied
E Hagatna	30	8	0.27	0.12	0.45	3.75	7.5(4.38)	13.76(4.98)	0.75	0.57	0.24	Varied
*Asan												
	30	4	0.13	0.09	0.71	7.50	11.14(4.99)	21.47(0.94)	0.67	0.6	0.11	heavily impacted
Cocos												
Lagoon	30	7	0.23	0.06	0.24	4.29	11.98(5.87)	16.54(13.5)	0.42	0.47	- 0.12	Best
Tumon												
Ypao Beach (S)	28	9	0.32	0.18	0.56	3.11	10.55(5.33)	17.86(4.6)†	0.83	1.00	- 0.20	recovering
Fujita Rd. (N)	26	12	0.46	0.18	0.38	2.17	11.07(5.2)	18.99(6.48)	0.81	0.88	- 0.09	recovering
Matapang (C)	27	11	0.41	0.15	0.38	2.45	8.34(4.05)	12.37(5.14)	0.79	0.78	0.01	recovering
Total Avg	29.1	8.1	0.28	0.13	0.50	3.95	9.96	16.31				
SD	1.5	2.3	0.10	0.04	0.15	1.48	3.77	6.34				

\*Grouped together for population genetic analyses

† excludes clone found in Tumon N plot which changes the clonal extent of that clone from 24.9 to 1446 m resulting in an average clonal extent of 302.51(640.91 sd) m.

<sup>1</sup>(Arnaud-Haond *et al.* 2007)

<sup>2</sup>(Porter *et al.* 2005, Burdick *et al.* 2008)

When pairwise comparisons from all plots were analyzed together, genetic distance was significantly autocorrelated with geographic distance for pairs of samples within 0-30 m, corresponding to the maximum distance within one circular sampling plot (radius =15m; Figure 16 <1.5 log(1+m)). The strength of correlation fell drastically at distances comparable to repeated plots within one site (Figure 16 classes 2.7 and 3; r=0.031 and -0.017 respectively; p<0.001 and 0.003) consistent with a well-mixed non-clonal population. At distances comparable to those between sampling sites, spatial autocorrelation was also



negligible ( $r=-0.053$  to  $-0.009$ ;  $p<0.001$ ). The same analysis excluding clones (shown in red Figure 16) resulted in significantly higher correlation at distances between 10 and 30m ( $r=0.039$  and  $0.061$ ;  $p<0.001$ ). However, the overall pattern of high correlation at the plot level in the analysis with clones was not mirrored indicating that the clonal subrange, or the linear distance over which clones affected the genetic structure of the population (described in Arnaud-Haond *et al.* 2007), extended over the entire range of the plot.

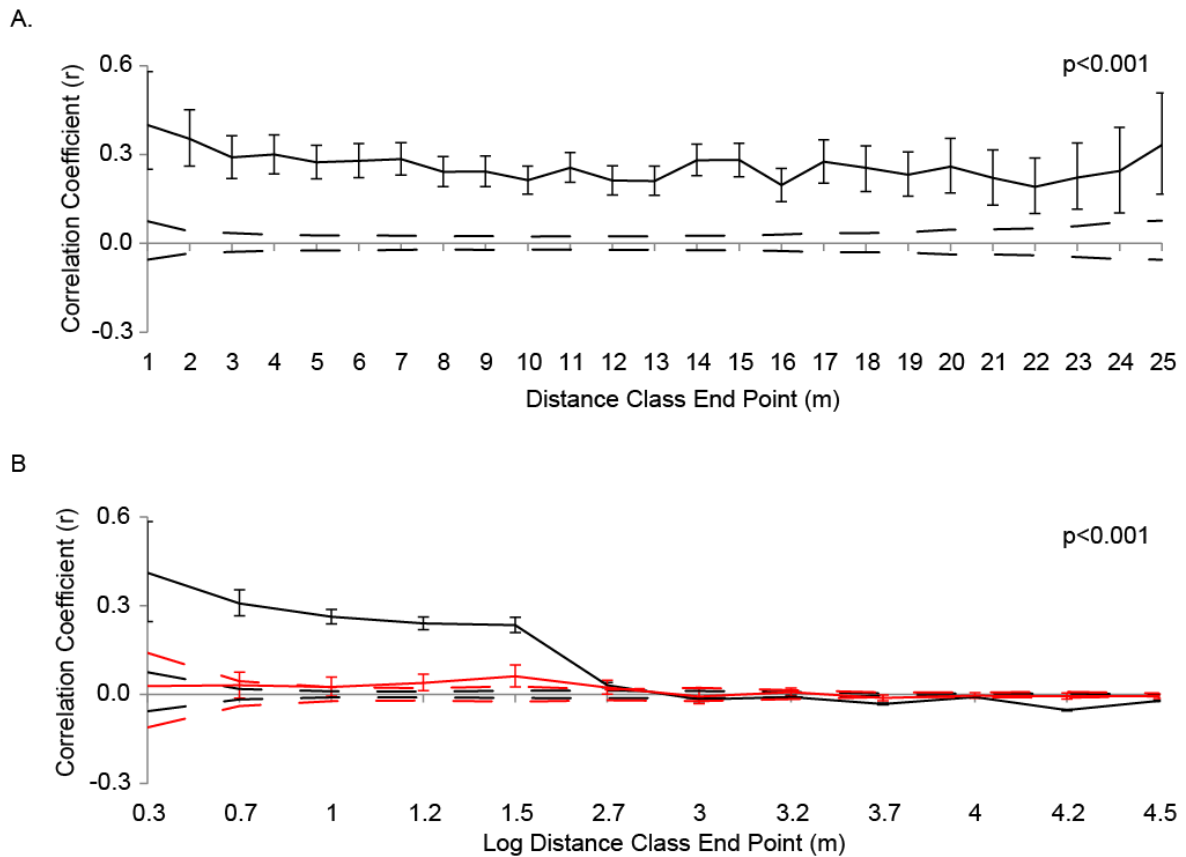


**Figure 16:** Correlogram depicting correlation between pairs of individuals within distance bins graphed against geographic distance given in meters (A) or  $\log(1+\text{meter})$  (B) between individuals (solid line). Dashed lines indicate 95% confidence intervals about the null hypothesis of no spatial genetic structure (i.e. genotypes are distributed randomly across geographic space). Correlograms are considered to be significant at  $p<0.01$  following (Banks & Peakall 2012). Black: with clones; Red: without clones

### Population Structure

Pairwise  $F_{ST}$  values revealed significant population structure (Table 5-6; Figure 17A) between Saipan and Guam as well as between Cocos at the southern tip of Guam and all other sites. Allele identity was similar overall in the Cocos samples compared to the rest of the population (no private alleles) but unusual alleles occurred at high frequencies and were likely responsible for the observed high  $F_{ST}$  values. Note, that the sample size was small (Cocos MLG=7; low allelic diversity) so these differences in allele frequencies were possibly exaggerated.

Results of Bayesian clustering including additional species indicated that despite high  $F_{ST}$  the Cocos samples were most likely *A. cf. pulchra*. The most likely number of clusters for the species analysis was  $K=3$ , with all *A. cf. pulchra* samples clustering together (Fig. 5-4B, top) and thus appropriate for population level analyses. At  $K=2$  (most likely via the Evanno method), MLGs from Cocos separated with high probability of membership to a second cluster, but Saipan and Tumon MLGs are not well resolved (Figure 17A, middle). At  $K=3$ , Saipan samples had high probability of membership into a third cluster but samples from Tumon assigned with equal probability to the first and third cluster (Figure 17B, bottom). Additionally, no isolation by distance pattern was observed (Mantel test; data not shown). **OBSTRUCT** to assessed the statistical significance of the **STRUCTURE** results at  $K=2$ , with a high  $R^2$  value of 0.88 ( $p < 0.001$ ) indicating strong diversification and/or population structure and thus rejecting the null hypothesis that ancestry is randomly scattered among the predetermined populations (Gayevskiy *et al.* .2014). After removal of each predefined population and recalculation of  $R^2$ , only removal of the Cocos population resulted in a decrease in  $R^2$  (from 0.88 to 0.77) indicating that Cocos alone contributed to an increase in structure and the rest of the data set was well mixed. This same pattern was followed when three inferred clusters were considered. Further, removal of the third inferred population resulted in an increase in  $R^2$  (+0.03) indicating that the third cluster was more homogenized than average and thus contributed less than average to the structure in the data (Gayevskiy *et al.* .2014). See the Supplemental material for this chapter for canonical plots of these data.

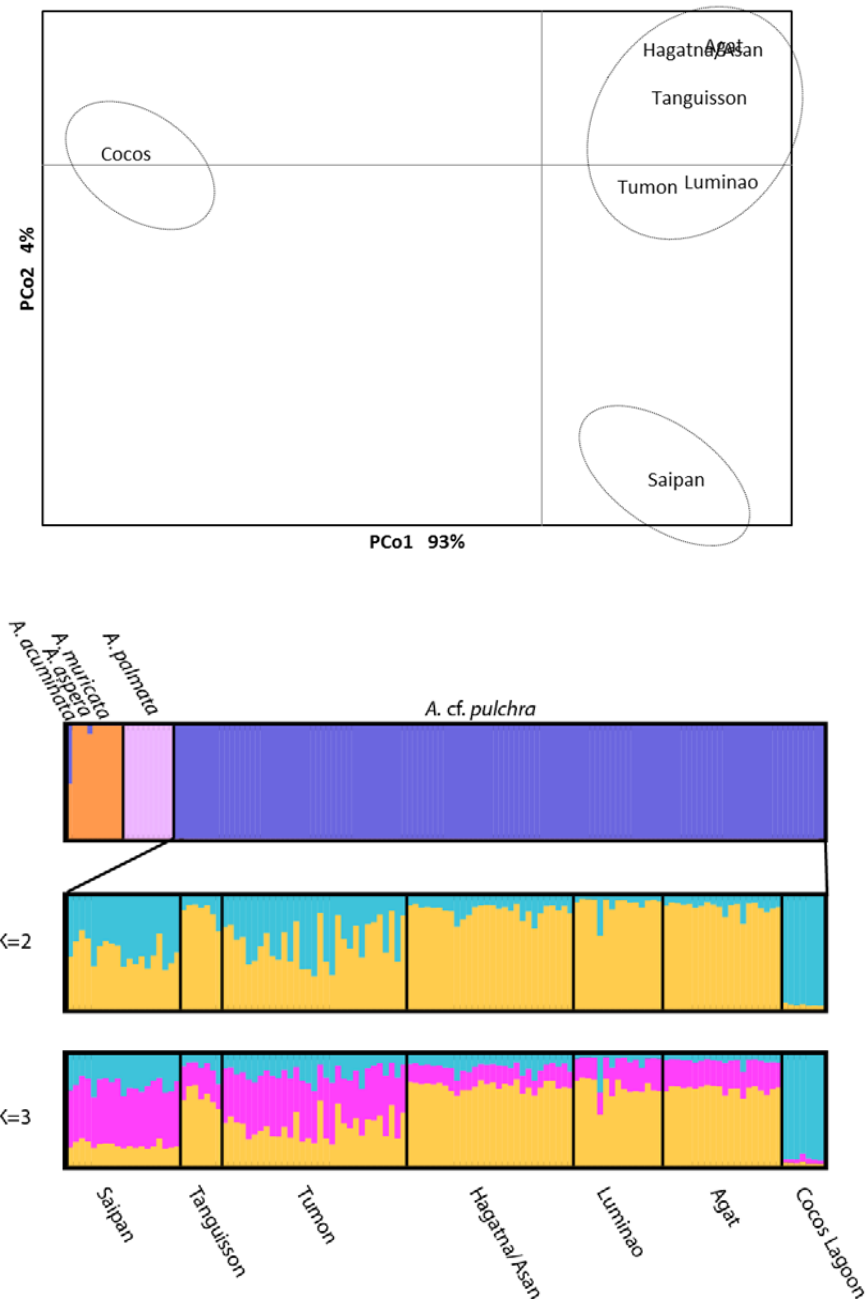


**Figure 17:** Principle coordinates analysis (PCoA) of pairwise  $F_{ST}$  distance matrix resulting in 3 clusters (A). The separation of Cocos Lagoon from the remaining sites given by PCo1 explains 93% of the variation in the data while the separation of Saipan from Guam given by PCo2 explains 4% of the variation. Solid circles represent clustering based on significant  $F_{ST}$  while the dashed circle represents most likely clusters based on Bayesian assignment. Results of Structure analyses (B) plotted as bar graphs of the probability of membership ( $y$ -axis;  $P_M$ ) to a given cluster for each individual along the  $x$ -axis. Top: No admixture model including multiple *Acropora* spp. gives  $K=3$  as most likely number of clusters with all *Acropora* cf. *pulchra* grouped as one cluster. Middle: The most likely number of clusters ( $K=2$ ) based on Evanno *et al.* method with Cocos having high probability of belonging to a second cluster and Saipan and Tumon samples unresolved. Bottom: Clustering assuming  $K=3$  based on  $F_{ST}$  results. Saipan has moderate probability of membership to a third cluster and Tumon is largely unresolved.

### **Migration modeling in MIGRATE**

For all configurations of populations (2, 3 or 4), the greatest support was shown for the unidirection model where migrants were passed to the next most northern site based on LogBayes Factor calculations (Table 4) consistent with the prevailing regional current (see *Discussion*). The number of migrants per generation ( $N_m$ ), calculated as  $\Theta^*(M/4)$ , estimated by this model are given in Table 4. Less than one migrant per generation was estimated from Cocos ( $N_m < 0.8$ ) under any population configuration and little support was shown for models allowing migration to Cocos. Under the two population scenario, grouping Guam and Saipan together,  $N_m$  from Cocos to Guam/Saipan was estimated to be 0.2. When Guam and Saipan were split into separate populations, there was a high amount of migration estimated from Guam to Saipan ( $N_m = 84.7$ ) consistent with on-going gene flow detected with STRUCTURE. Migration rates from Cocos to Guam remained the same. When sampling sites were grouped into four population groupings: Cocos; mid-Guam –Agat, Luminao, Hagatna, and Asan; north-Guam – Tumon and Tanguisson; and Saipan, the model gave the greatest likelihood score. Migration was strong in the northward direction with the exception of little migration from Cocos ( $N_m = 0.8$ ).

**Table 4:** Log Bayes factors (2\* difference in log-likelihood) based on Bezier approximation score (a) and the estimated number of migrants per generation (b-d) calculated as the median estimated mutation-scaled population size ( $\Theta$ ) x the median estimated mutation-scaled migration rate / 4. The most likely model (N) for each configuration of populations is underlined. N = northward migration, S = southward migration, N + Cocos to NG = a channel of migration from Cocos to northern Guam sites in addition to southern Guam, 0 Cocos = full model except no migration to and from Cocos Lagoon, 0 Saipan to S = full model but no migration from Saipan to the south.

a)

Migration Model	Number of Populations		
	2	3	4
Full	-33427	-55608	-
N	<u>-6341</u>	<u>-4742</u>	<u>0</u>
S	-11027	-5814	-679
N+Cocos to NG	-	-	-869
0 Cocos	-	-120730	-
0 Saipan to S	-	-39542	-

b) Two populations

Number of Migrants per Generation

		Receiving Population	
$\Theta$	Source Population	Saipan/Guam	Cocos L.
7.7	Saipan/Guam	-	-
0.8	Cocos L.	0.2	-

c) Three populations

Number of Migrants per Generation

		Receiving Population		
$\Theta$	Source Population	Saipan	Guam	Cocos L.
1.6	Saipan	-	-	-
6.8	Guam	84.7	-	-
0.8	Cocos L.	-	0.2	-

d) Four populations

Number of Migrants per Generation

		Receiving Population			
$\Theta$	Source Population	Saipan	North Guam	Mid Guam	Cocos L.
1.6	Saipan	-	-	-	-
39.6	North Guam	556.9	-	-	-
6.1	Mid Guam	-	57.7	-	-
2.23	Cocos L.	-	-	0.8	-



## ACROPORA AS FISH HABITAT

**Table 5:** Total number of fish species recorded during a stationary point count inside (In) and outside (Out) staghorn patches in Tumon, Agat and East Agana. Nd = no data.

Location	Replicate	# species
Tumon	In1	24
Tumon	In2	21
Tumon	In3	18
Tumon	Out1	15
Tumon	Out2	21
Tumon	Out3	16
Agat	In1	31
Agat	In2	26
Agat	In3	32
Agat	Out1	21
Agat	Out2	24
Agat	Out3	nd
East Agana	In1	14
East Agana	In2	14
East Agana	In3	13
East Agana	Out1	12
East Agana	Out2	11
East Agana	Out3	12

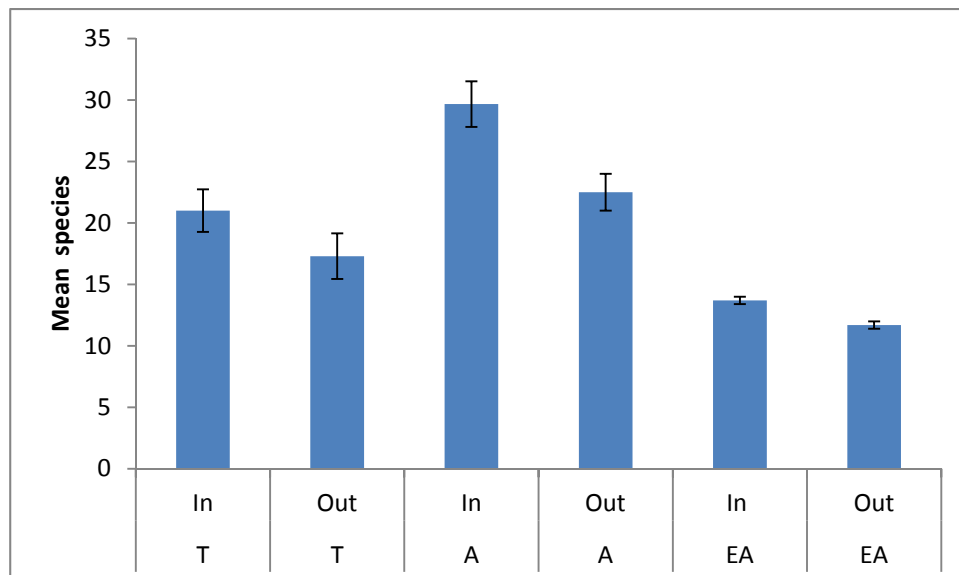


**Figure 18:** Mean number fish species inside (In) and outside (Out) of Acropora patches in each of three locations; Tumon (T), Agat (A) and East Agana (EA).

Fish were counted on a 10 min stationary count within a 5 m radius. All species encountered during this time were recorded as present (Table 5). Underwater visual census reveal *Acropora* patches comprised a similar fish assemblage to that of adjacent reef flat habitat ( $p=0.06$ , T-test,<sub>2</sub>)(Figure 18). Mean species richness was greatest in *Acropora* patches at Agat where 30 species were recorded. Inside the staghorn patches at East Agana by comparison had fewer number of species compared with Tumon and Agat or 34% and 54% fewer respectively.

## **PATTERNS OF DISPERSAL AND CONNECTIVITY**

### **Model Development**

The basic advection-dispersion model used to track coral larvae in this project has previously been described by Wolanski et al. (1997) with a more detailed explanation contained within McIlwain and Halford (2010). A similar model was also used to examine coral connectivity in Palau (Golbuu et al 2012). It is a Lagrangian model that follows released particles, with diffusion simulated by a random Markov walk along exactly curved streamlines. For each scenario we specified the location (as cell positions), concentration of particles and larval duration from multiple release points, either simultaneously or separately. Larvae were assumed to be passive propagules. The current regime used for the model was typical for low to medium ENSO values with a far-field current of  $0.1 \text{ ms}^{-1}$  running from East to West.

Extensive mapping identified the location and spatial extent of all significant *Acropora pulchra* thickets around Guam. The total area occupied by *A. pulchra* within each bay was used as a relative measure of larval propagule numbers that could be released from each bay during spawning season. Using this relationship the number of propagules released from each bay is provided in Table 6 and Figure 19.

**Table 6:** The spatial extent of adult *A.pulchra* colonies in each of the 7 locations derived from the satellite images. The total area was used as a relative measure of the numbers of propagules released from each location before the bleaching event (Pre-bleaching) and after the bleaching event (Post-bleaching). The approximate mortality as a result of the bleaching is given in parenthesis (Burdick pers.obs).

<b>Location</b>	<b>Spatial Extent (m<sup>2</sup>)</b>	<b>Pre-bleaching**</b>	<b>Post-bleaching***</b>
Tanguisson	6 482	6 500	(50%) 3 250
Tumon	150 056	150 000	(60 %) 60 000
Agana*	64 372 + 27 952	65 000, 30 000	(75 %, 25 %) 16 250, 22 500
Governors (Adelup)	3 221	3 500	3 500
Agat	43 309	45 000	(50 %) 22 500
Cocos	506	1 000	1 000
Ipan (Togcha)	5 035	5 000	5 000

\* There were 2 very separate locations at either end of the greater Agana Bay area and hence these were treated as separate populations for the model runs.

\*\* The number of propagules released from each location for the initial model run.

\*\*\* The number of propagules released after the bleaching mortality events. The values in parenthesis represent the qualitative estimates of bleaching mortality that occurred at each location.

There are no published estimates of effective larval duration for *A. pulchra* around Micronesia therefore the general literature on *Acropora* larval durations was used as a guide (e.g. Baird et al 2009; Golbuu et al. 2012). The majority of larval settlement was assumed to have occurred within 3-5 days of spawning with a significantly decreasing settlement rate after this period. Model output was the result at 5 and 10 days by which time the majority of larval settlement should have occurred. Runs of 20 days were included only to demonstrate the ultimate fate of unsettled coral larvae.

The model was run with a simultaneous release of propagules from each of the 7 locations, followed by a site- by- site larval release to enable patterns of source and supply to be elucidated. This pattern was repeated for the post-bleaching data to see the effects of large mortality events on the longer-term viability of *A. pulchra* population around Guam.

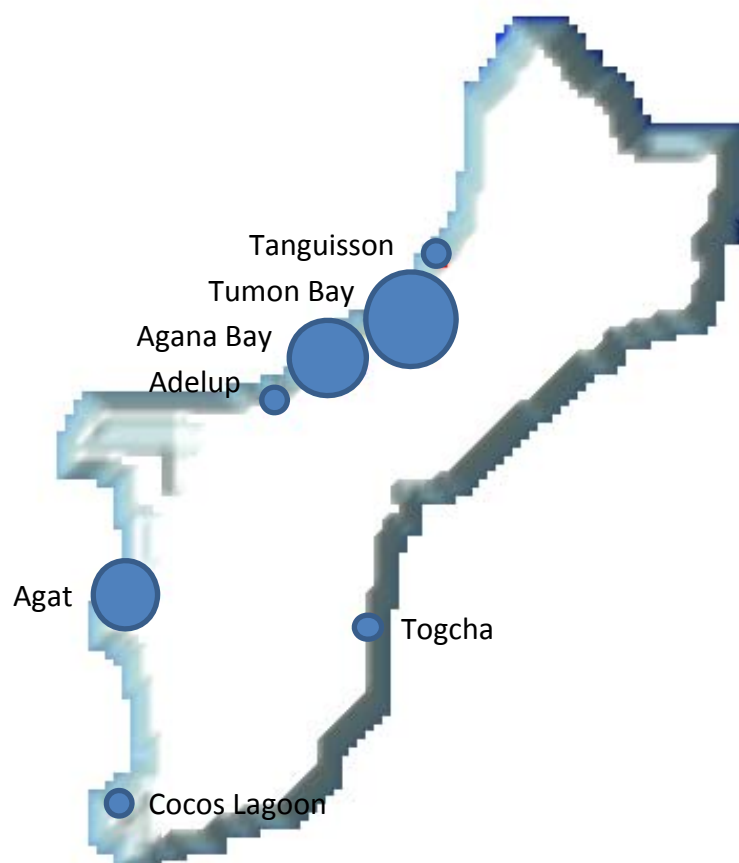


**Figure 19:** Map showing that the total propagules released from each of the 7 locations is proportional to the total area of *Acropora* found at each location.

### **Biophysical modelling output**

The output from the larval dispersal model show that after only 12 hours following spawning, a large proportion of the larvae are retained close to their release point (Figure 20A). By five days post-spawning the greatest settlement occurs around the three areas with the highest abundance of *A.pulchra*; that of Tumon Bay, Agana Bay and Agat (Figure 20B). After that time larvae spawned from Guam's east coast (e.g. Togcha) are dispersed to the south with little or no chance of settlement. By the tenth and twentieth day post-spawning, the majority of larvae spawned from Togcha and Cocos Lagoon have been dispersed to the west of Guam with little or no evidence of settlement taking place (Figure 20 C,D).

When larvae are released from each of the four main study sites (Tumon, Agana, Agat and Cocos) separately, their individual contributions to settlement patterns around Guam become clear. After five days, when the majority of coral larvae have settled, propagules from the two northern locations, Tumon and Agana were retained along the northwest coast of Guam with little or no dispersion to the south (Figure 21A,B). The Agat population of *A.pulchra* produced larvae that only dispersed along the southwest coast with no larvae settling north of Orote Point although a small percentage did settle in the northern part of Cocos Lagoon (Figure 21 C). Larvae released from Cocos, however were advected away from the coast making no contribution to the settlement of *A.pulchra* along the west coast (Figure 21D).

During the summer months of 2014, a bleaching event occurred on Guam that significantly impacted the adult thickets of *A.pulchra*. This gave us the opportunity to run our anticipated modelling scenarios as "real" events. We found that when adult *A.pulchra* mortality was reduced by up to 70% (the approximate loss due to the bleaching), larval settlement was heavily impacted but proportional to the loss of adults (Figure 22B).

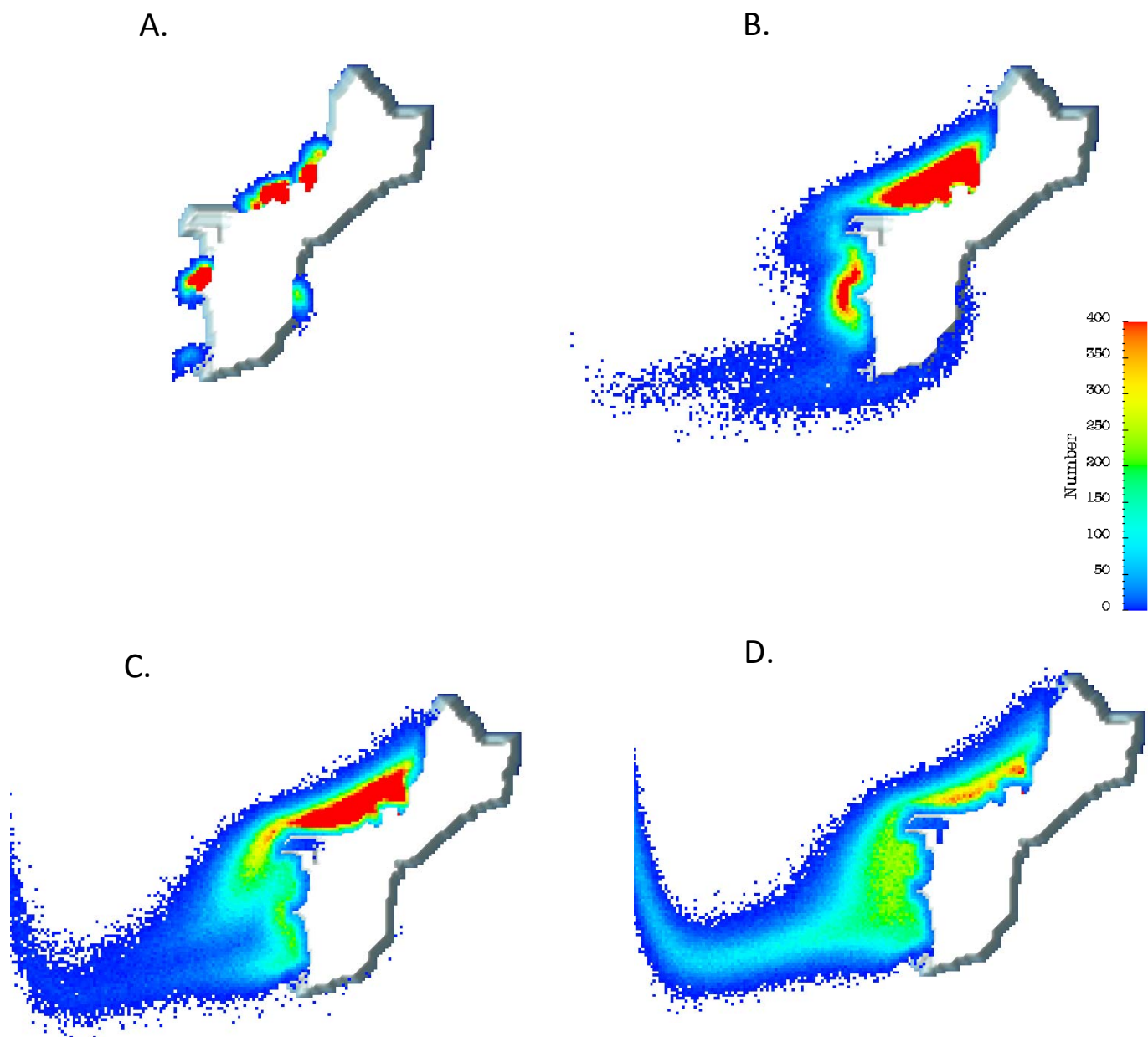


**Figure 20:** An example of output from a series of model runs on the dispersal patterns of *A. pulchra* larvae released from 7 locations around Guam simultaneously. Pelagic Larval Duration A) 12 hours; B) 5 days; C) 10 days; D) 20 days. The basic model parameters for these runs were Boundary 1: Tides were represented by a Cosine function with 2 high and 2 low tides each 24 hr cycle; Boundary 2 & 4: Mean North-South Current speed  $0.008 \text{ ms}^{-1}$ ; Boundary 3: Mean East-West Current speed  $0.1 \text{ ms}^{-1}$ ; Mean larval swimming speed  $0 \text{ ms}^{-1}$ ;



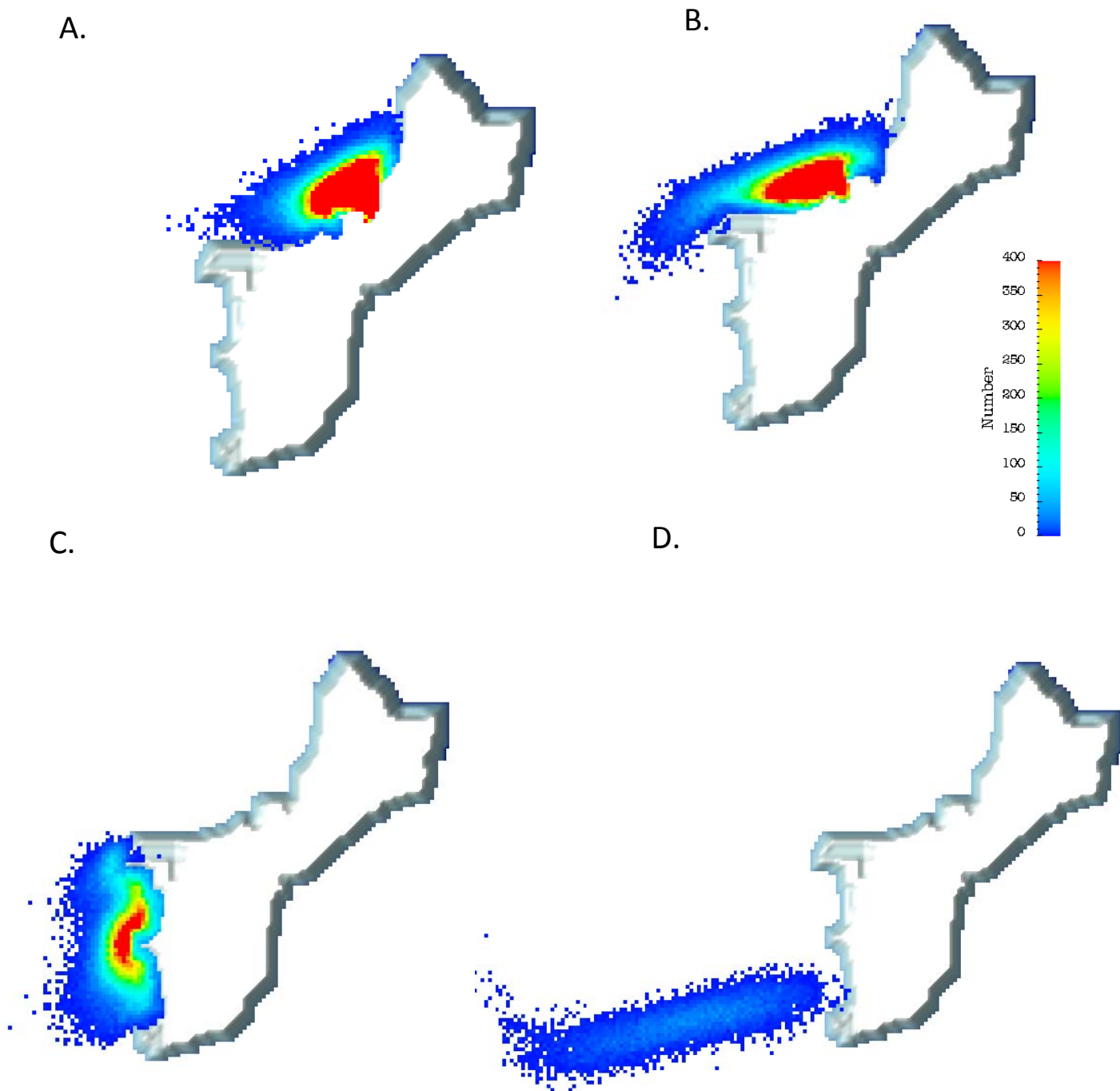


**Figure 21:** An example of output from a series of model runs on the dispersal patterns of *A. pulchra* larvae released from 4 locations around Guam separately. Pelagic Larval Duration 5 days which is when the majority of coral larvae have settled for A) Tumon Bay; B) Agana Bay; C) Agat; D) Cocos Lagoon. The basic model parameters for these runs were Boundary 1: Tides were represented by a Cosine function with 2 high and 2 low tides each 24 hr cycle; Boundary 2 & 4: Mean North-South Current speed  $0.008 \text{ ms}^{-1}$ ; Boundary 3: Mean East-West Current speed  $0.1 \text{ ms}^{-1}$ ; Mean larval swimming speed  $0 \text{ ms}^{-1}$ ;

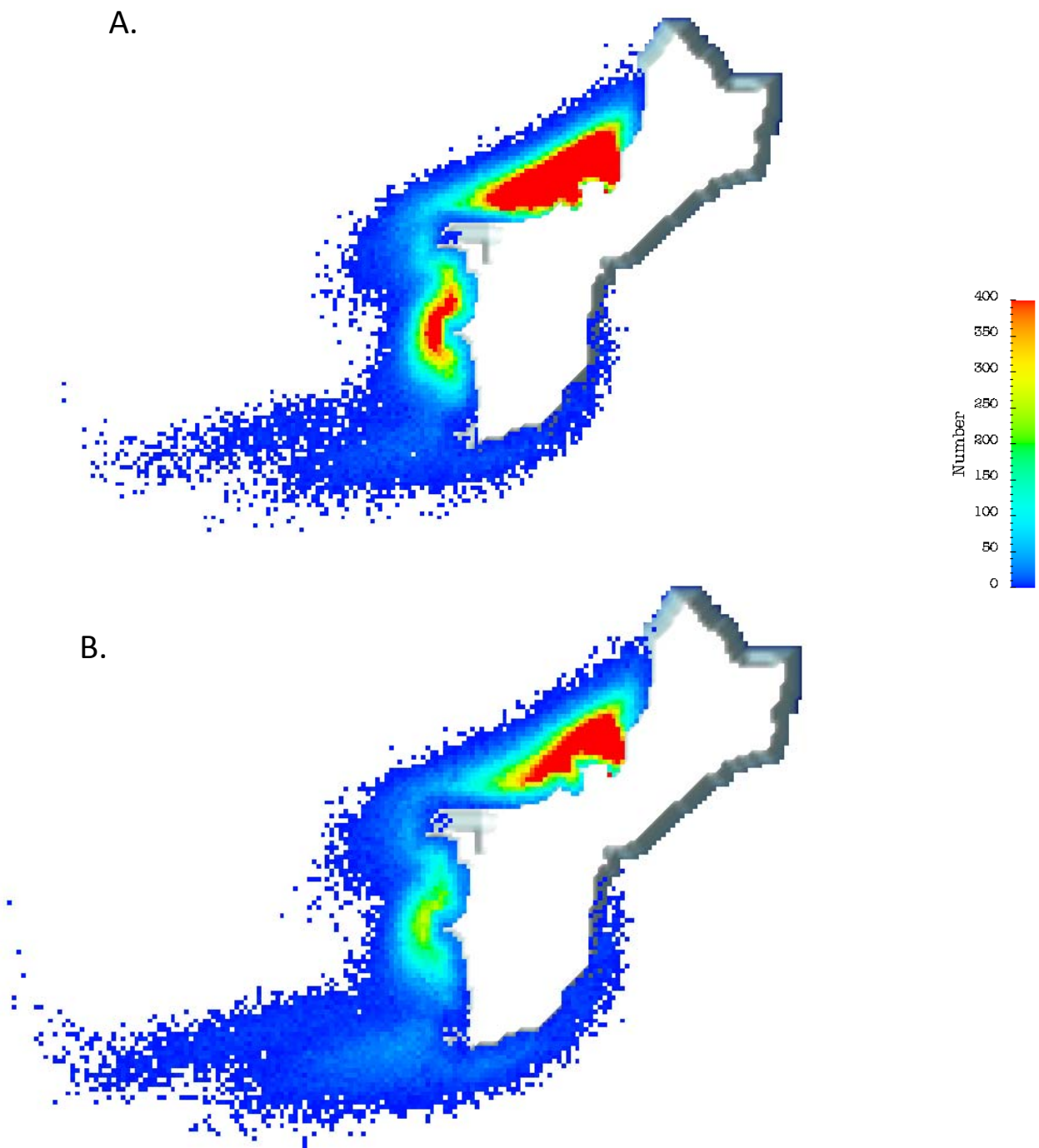


**Figure 22:** An example of output from a series of model runs on the dispersal patterns of *A. pulchra* larvae from 7 locations around Guam with a pelagic Larval Duration 5 days; A) before and B) after a major bleaching event with approximately 70% mortality of adult colonies. The basic model parameters for these runs were Boundary 1: Tides were represented by a Cosine function with 2 high and 2 low tides each 24 hr cycle; Boundary 2 & 4: Mean North-South Current speed  $0.008 \text{ ms}^{-1}$ ; Boundary 3: Mean East-West Current speed  $0.1 \text{ ms}^{-1}$ ; Mean larval swimming speed  $0 \text{ ms}^{-1}$ ;